



SACLANT ASW
RESEARCH CENTRE
REPORT

AN EVALUATION OF DIGITIZED APT DATA
FROM THE TIROS-N/NOAA-A,-J SERIES
OF METEOROLOGICAL SATELLITES

by

Brian WANNAMAKER

15 March 1984

NORTH
ATLANTIC
TREATY
ORGANIZATION

LA SPEZIA, ITALY

This document is unclassified. The information it contains is published subject to the conditions of the legend printed on the inside cover. Short quotations from it may be made in other publications if credit is given to the author(s). Except for working copies for research purposes or for use in official NATO publications, reproduction requires the authorization of the Director of SACLANTCEN.

This document is released to a NATO Government at the direction of the SACLANTCEN subject to the following conditions:

1. The recipient NATO Government agrees to use its best endeavours to ensure that the information herein disclosed, whether or not it bears a security classification, is not dealt with in any manner (a) contrary to the intent of the provisions of the Charter of the Centre, or (b) prejudicial to the rights of the owner thereof to obtain patent, copyright, or other like statutory protection therefor.

2. If the technical information was originally released to the Centre by a NATO Government subject to restrictions clearly marked on this document the recipient NATO Government agrees to use its best endeavours to abide by the terms of the restrictions so imposed by the releasing Government.

Published by



SACLANTCEN REPORT SR-78

NORTH ATLANTIC TREATY ORGANIZATION

SACLANT ASW Research Centre
Viale San Bartolomeo 400, I-19026 San Bartolomeo (SP), Italy.

tel: $\frac{\text{national} \quad 0187 \ 560940}{\text{international} + 39 \ 187 \ 560940}$
telex: 271148 SACENT I

AN EVALUATION OF DIGITIZED APT DATA FROM THE TIROS-N/NOAA-A,-J SERIES
OF METEOROLOGICAL SATELLITES

by

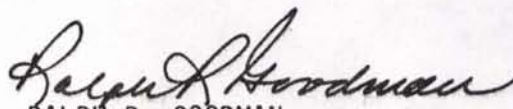
Brian Wannamaker

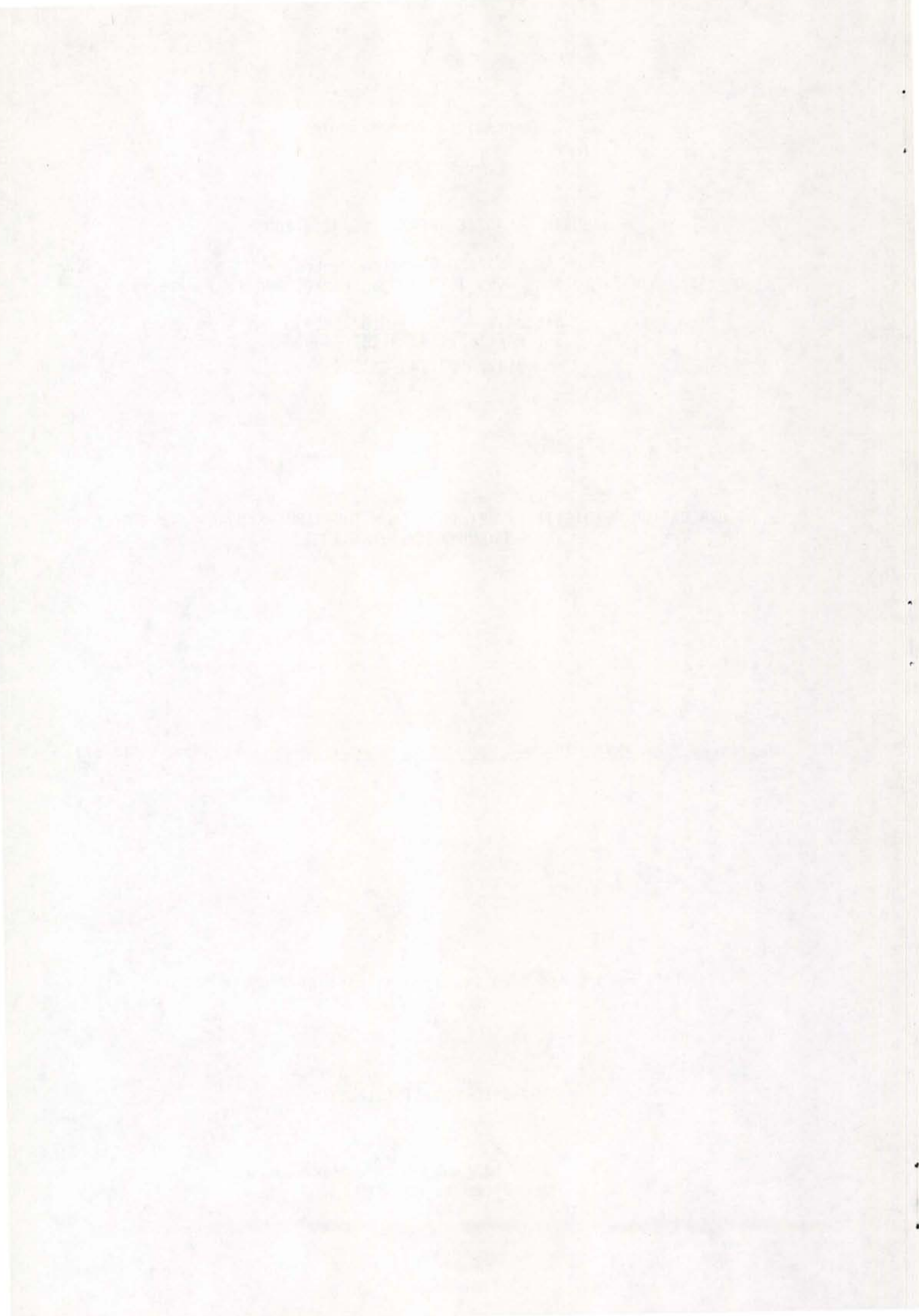
(Reprinted from International Journal of Remote Sensing 5, 1984: 133-144)

15 March 1984

This report has been prepared as part of Project 01.

APPROVED FOR DISTRIBUTION


RALPH R. GOODMAN
Director



An evaluation of digitized APT data from the TIROS-N/NOAA-A, -J series of meteorological satellites

BRIAN WANNAMAKER

NATO SAACLANT ASW Research Centre, Viale San Bartolomeo 400,
19026 La Spezia, Italy

(Received 13 September 1983)

Abstract. The TIROS-N/NOAA-A, -J series of meteorological satellites transmit imagery data to the Earth in both digital and analogue formats. The analogue data are a processed subset of the digital data and have lower resolution. A quantitative evaluation of a post-reception digitized version of this is made using the corresponding digital data as a standard. In nine comparisons the calibration of the infrared sensor on board was within 0.01°C. Sea surface temperature estimates from APT data were 0.3°C below the corresponding digitally transmitted data. The albedo estimates were within 0.2 per cent. Processed APT data are adequate for many mesoscale measurements in the fields of oceanography and meteorology and are more readily accessible than the digitally transmitted data.

1. Introduction

The imagery data from meteorological spacecraft have been increasingly applied to oceanographic research as data quality has improved. A significant step forward in this improvement was the new instrument on the TIROS-N/NOAA-A, -J series. Noise was virtually eliminated from the data by the use of digital transmission and the multiple channels of thermal infrared information allowed improved sea surface temperature estimates to be made.

Also improved on this spacecraft series were the APT (Automatic Picture Transmission) formatted data. The APT data have been available to relatively low cost portable receiving stations since 1963. APT initially supplied only visible, photographic data, but thermal infrared data were added in 1972. The ease of reception has been at the expense of resolution. This data format has served a large number of meteorologists and thousands of amateurs with cloud pictures extensively used for nephanalysis and weather forecasting (for example, Zwatz-Meiss 1981). The infrared (I.R.) data were sufficient to show strong sea surface temperature gradients and were used in oceanographic experiments as surveyed by La Violette *et al.* (1975). On the TIROS-N satellite the APT data become a digitally processed product of the main high-resolution sensor. The spatial and temperature resolution was improved, transmission bandwidth was increased, and the antenna was made more efficient. These changes promised to justify increased ground processing of the data into quantitative products for use in oceanographic research.

This report discusses the quality of digitized APT data, taking the full resolution, digitally-transmitted data as the standard. The data are evaluated for their ability to return precise geophysical parameters at known geographical positions. The APT

format and the data base used for the comparison is first outlined, and this is followed by a discussion of the results and conclusions. It is shown that the quality is sufficient for many mesoscale measurements.

2. The data

The Advanced Very High Resolution Radiometer (AVHRR) on board the satellites supplies five channels of data: visible, near infrared, and three in the thermal infrared. Some satellites in the series carry instruments with only four channels. Details are given in Schwalb (1978, 1982). The digitized output of the AVHRR is combined with data from other information and transmitted digitally to stations within line of sight. This is the HRPT format (High Resolution Picture Transmission). The subsatellite spatial resolution is about 1.1 km and the noise equivalent differential temperature of the infrared channels is less than 0.12°C at 27°C.

The APT format is a subset of this. Every third line of two of the channels is selectively averaged in an on-board digital processor, the MIRP. This averaging is designed to remove the effects of the Earth's curvature in the imagery, creating a nominal along-scan resolution of 4 km. Five averaging schemes are used. At the centre of the scan four adjacent pixels are averaged; at the ends of the scans the resolutions of APT and HRPT formats are equal. The two averaged channels are converted to analogue signals, time multiplexed along with calibration data and are amplitude modulated on to a 2.4 kHz carrier, which is in turn FM modulated on to 137 MHz. These data may be received on board ships with omnidirectional antennas. The data discussed below were obtained with a directional Yagi-type antenna at a station situated on the north-west coast of Italy.

The form of the imagery is shown in figure 1, which is a near-infrared image of western Europe on 9 July 1982. The image from a northbound pass has been inverted to depict north at the top; thus reception time increases from right to left and bottom to top. Along the right side is a series of vertical bars indicating the channel synchronization pulse on each line. Following this is a dark stripe of space data, a value corresponding to the sensor output when viewing deep space. This is broken every minute (120 lines) by markers. Along the trailing edge of the image is a repeating series of 16 grey-scale steps, each eight lines deep, of calibration data. The FM demodulated data were digitized at twice the AM carrier frequency, accomplishing demodulation and doppler shift removal from the incoming signal. The relation between pixel position along a scan line in the original sensor output (and HRPT data format) and in the digitized APT data is shown in figure 2. The APT data are some 15 per cent oversampled; this shows clearly at the ends of the lines, where there are more samples than there were in the sensor output. The digitization is to 10 bits (levels 0 to 1023).

Figure 3 shows a portion of the data of the same orbit as Figure 1 but from the HRPT formatted data. The area shown is the western Mediterranean on 9 July 1982. The distortion near the edges of the image is very evident compared to figure 1.

To evaluate the quality of the APT data, HRPT data were taken to represent the true output of the AVHRR. A direct comparison was made between the APT-formatted data received directly and the HRPT-formatted data obtained on computer-compatible tapes from the University of Dundee Receiving Station. Data, which had been selected as part of other research, were taken from nine passes of the NOAA-7 satellite made between 23 June and 27 July 1982.

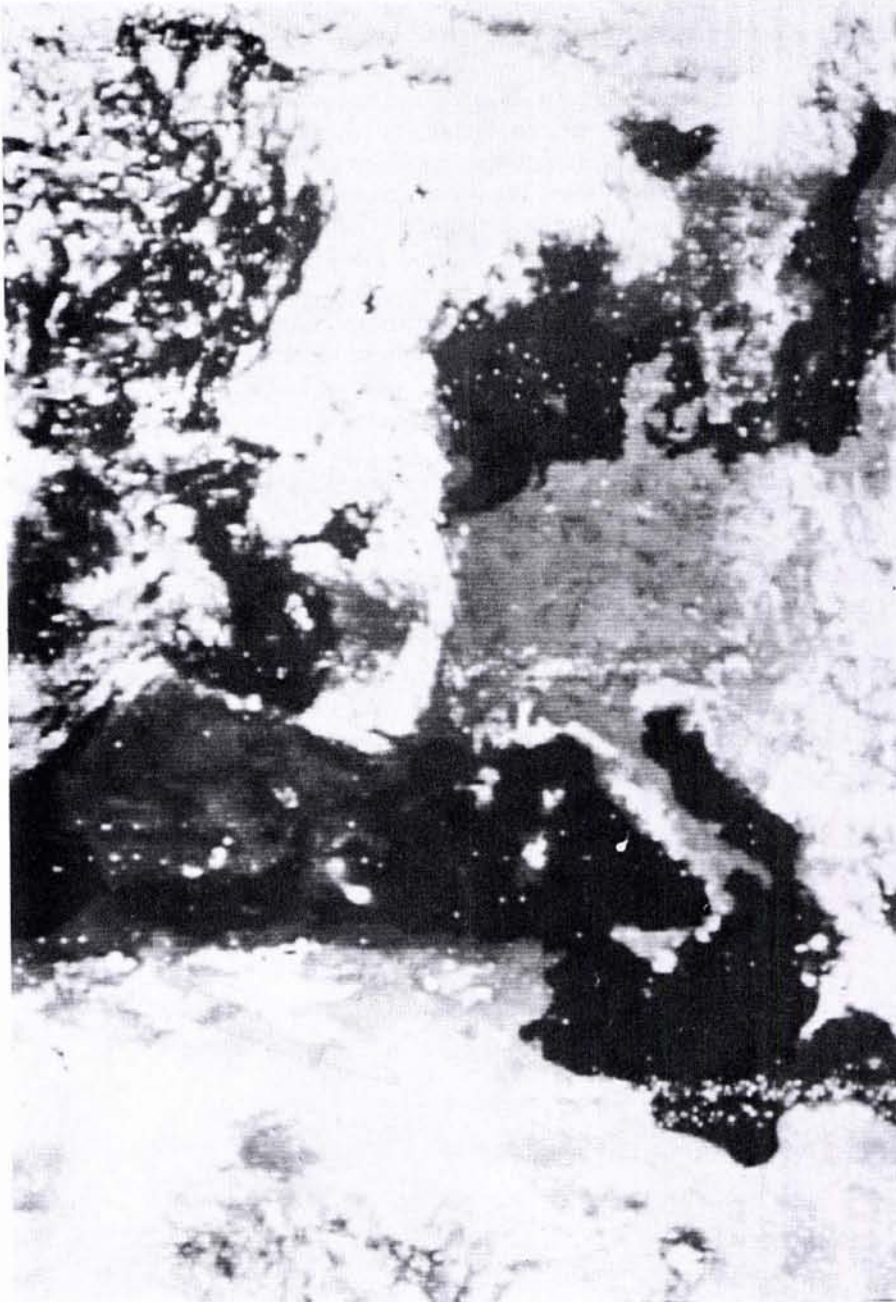


Figure 1. Near-I.R. image of western Europe on 9 July 1982 from digitized APT transmission. The image has been inverted to show north at the top. Data acquisition began in the lower right corner. The image is subsampled 3×3 for the display.

The procedure for converting digital HRPT data into geophysical parameters is discussed by Lauriston *et al.* (1979). The first stage in the procedure for APT data is then to develop a model to estimate the corresponding HRPT value given an APT value. For geographical corrections this must consider the selective averaging done in the MIRP. For the albedo or temperature levels this must include any non-linearities in the transmission path, especially in the modulation/de-modulation and recognize that noise has been added during the transmission. Nine of the 16 grey-scale steps represent constant modulation levels injected on board the satellite. Once these levels were determined from the data received they were used to estimate an orthonormal fifth-degree polynomial relationship between an APT and HRPT count value. The constant modulation levels are repeated about ten times during a full satellite pass. The least noisy values for each step were used for the curve fitting to avoid noise contamination. The value for each step was the average of over 300 samples and the standard deviation of the final estimates was generally less than 0.1 count. The polynomial determined was then used to convert the other calibration step values to equivalent HRPT values and calibration proceeded from there as for the HRPT data.

The visible and near-infrared sensors have no in-flight calibration updates. The infrared channels can be calibrated at two points along the curve of radiance against counts many times during a scene. On every scan the AVHRR views deep space and a black body inside its housing. The temperature of the black body is actively maintained at about 15°C and is separately measured by four platinum resistance thermometers distributed over its surface. A consistent variation in the temperatures of about 1°C was reported by the thermometers. This should not affect the calibration if the average of the four thermometers adequately models the temperature of the portion of the black body in view of the sensor during the back scan. This temperature

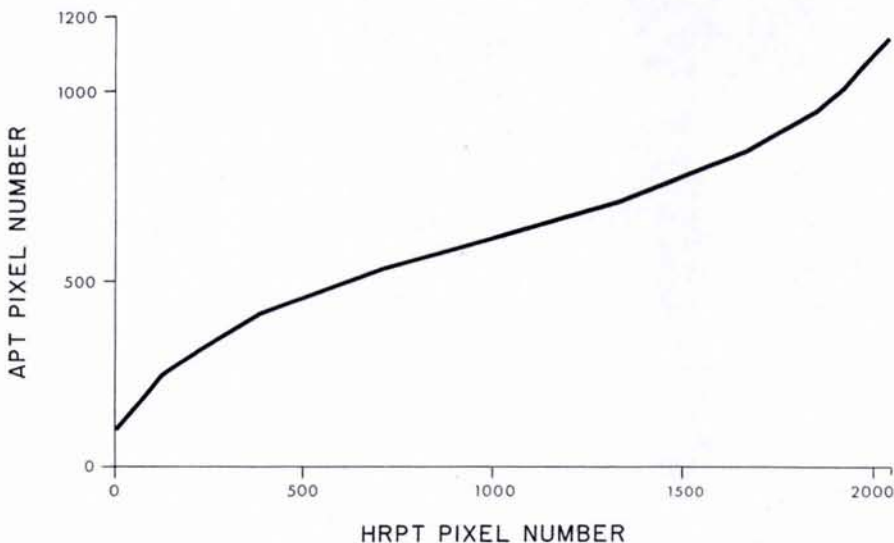


Figure 2. The relationship between the along-scan-line positions of corresponding pixels in the digital HRPT and in the APT format digitized at 4.8 kHz.

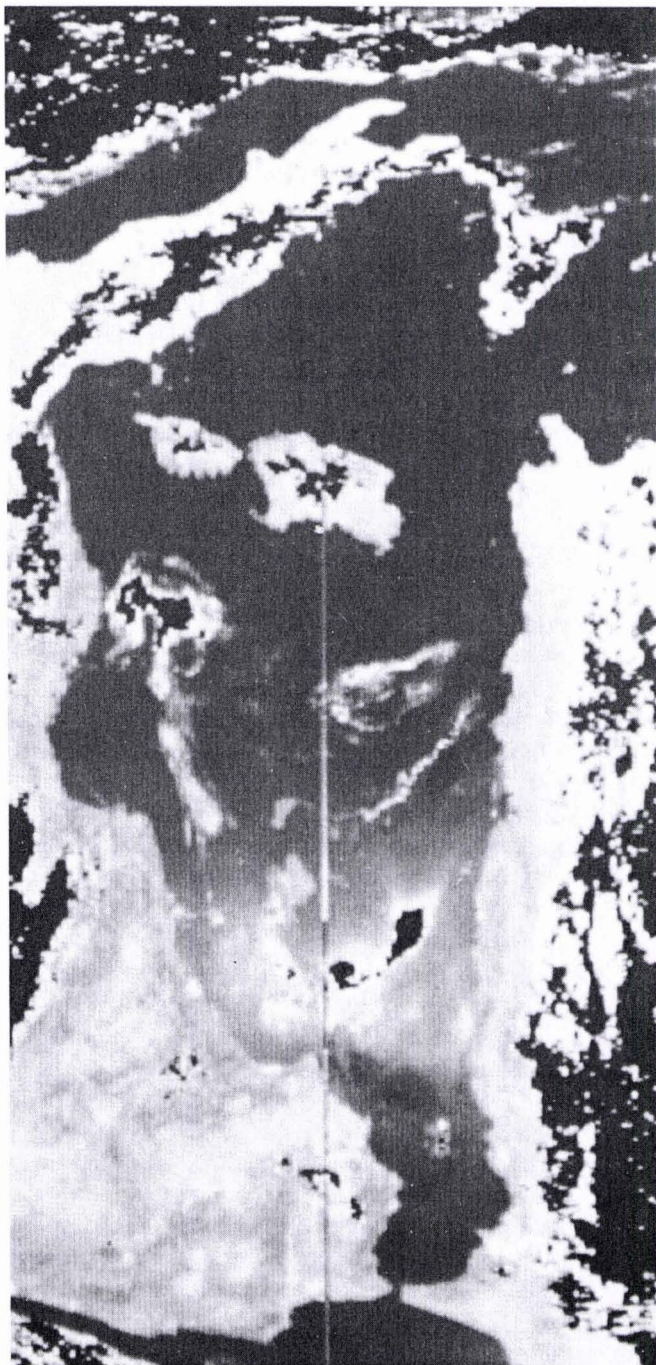


Figure 3. Near-I.R. image in HRPT format during the same orbit as in figure 1. The image is shown subsampled 4×4 .

variation, which has also been noted in TIROS-N and NOAA-6 data, may have been due to heat leakage from other portions of the spacecraft or reflected solar radiation. The average temperature during night passes was about 1.5°C lower but the variation between thermometers remained. The temperature of the black body is converted to an equivalent radiance by considering the sensor response function and the Planck function. The thermometers and back-scan values are reported on every line of the HRPT data and as grey-scale wedges in the APT data every 128 lines.

The response of the sensors of channel four and five are slightly non-linear. To minimize the effect of this while maintaining a linear calibration curve, the pre-launch calibration data were fitted to a line over the temperature range of -48°C to 32°C . This line was then extrapolated to give an artificial space radiance value. This value is supplied by NASA through NESDIS (Lauriston *et al.* 1979).

With the four values of blackbody radiance, the artificial space radiance, and the sensor output when viewing the black body and space, the gain and intercept of the calibration line between the sensor output and received radiance were calculated (table 1).

To illustrate the effects of the differences in calibration parameters estimated from the two data sets, a count value of 360 was converted to the corresponding radiance (R_{360}) and temperature (T_R) values in all cases. The value of 360 was chosen because it translates into a temperature within the range of expected sea surface temperature values. The results are shown in table 1. T_L was the value resulting from modelling the conversion from APT to HRPT count values by a least-squares linear fit rather than by the polynomial discussed above.

Once the sensor was calibrated, the count value for every pixel in the images could be converted to a value representing the temperature or albedo at the top of the atmosphere. Equally important is the geographical position of each pixel, so that the sizes of sea surface features and their movement from one image to another can be measured.

The geographical calibration of the image was approached with a knowledge of only the nominal values of the satellite's orbit parameters. An interactive input of ground control points was used to build up a time series estimator of the spacecraft motion (Orth *et al.* 1978, Caron and Simon 1975). From this, a new image can be created on a standard map projection.

For a further comparison of the positional and geophysical parameter accuracy of the data types, the afternoon orbit of 9 July 1982 was chosen. The ascending node was at 16.7°E . The area of the western Mediterranean was generally cloud free with a sun-glint pattern south of the Balearic Islands. The two near-infrared images are shown in figures 1 and 3. Ground-control points from an area bounded by 3°W to 14°E and 35° to 44°N were used, 11 for the HRPT and 12 for the APT images. The residual r.m.s. errors between the positions of the control points estimated by the operator and the algorithm were 1.6 and 4.7 km for the high and medium resolution data respectively. The poorer resolution of the APT images makes it more difficult to locate ground-control points interactively on the monitor screen. Since only every third line of the original data was used for the resolution APT format some small control points did not even exist in the medium resolution data. The four images (two near-I.R., two thermal I.R.) were each mapped to a Standard Mercator projection with a scale of 4 km/pixel at 41°N .

Figure 4 is a pixel-by-pixel difference between the two mapped and calibrated thermal images with an offset of 18°C . The contrast stretch is 3°C from black to

Table 1. A comparison of calibration data and calculated results from the data transmissions in APT (above) and HRPT formats (below).

Orbit	Date	Ascending node time (G.M.T.)	Black body temperature (°C)	Back scan (counts)	Space data (counts)	Gain	Intercept ($\times 10^{-3}$)	R_{360}	T_R (°C)	T_L (°C)
5153	23/6	1327	15.59 15.75	373.67 372.85	996.03 991.97	-0.15400 -0.15500	0.15223 0.15261	96.79 98.81	17.11 17.13	17.46
5223	28/6	1226	15.51 15.55	373.50 373.91	995.21 992.03	-0.15410 -0.15500	0.15214 0.15256	96.66 96.76	17.03 17.09	17.53
5231	29/6	0202	14.23 14.13	386.11 385.86	992.85 992.04	-0.15544 -0.15439	0.15216 0.15198	96.20 96.40	16.73 16.86	17.44
5266	1/7	1332	15.64 15.69	373.05 372.53	998.02 992.03	-0.15350 -0.15501	0.15198 0.15260	96.72 96.80	17.07 17.12	17.62
5379	9/7	1338	15.65 15.66	373.46 372.95	996.25 992.05	-0.15404 -0.15502	0.15228 0.15261	96.83 96.80	17.14 17.12	17.62
5393	10/7	1325	15.58 15.67	372.83 373.65	996.99 992.04	-0.15350 -0.15488	0.15188 0.15247	96.62 96.71	17.00 17.06	17.50
5548	21/7	1254	15.37 15.57	373.52 373.69	978.20 992.05	-0.15790 -0.15500	0.15331 0.15254	96.45 96.74	16.90 17.08	17.51
5556	22/7	0230	14.25 14.23	385.34 384.91	995.34 992.02	-0.15330 -0.15440	0.15139 0.15202	96.20 96.44	16.73 16.88	17.30
5633	27/7	1324	15.46 15.64	372.67 372.97	997.41 991.98	-0.15320 -0.15500	0.15164 0.15256	96.49 96.76	16.92 17.09	17.47

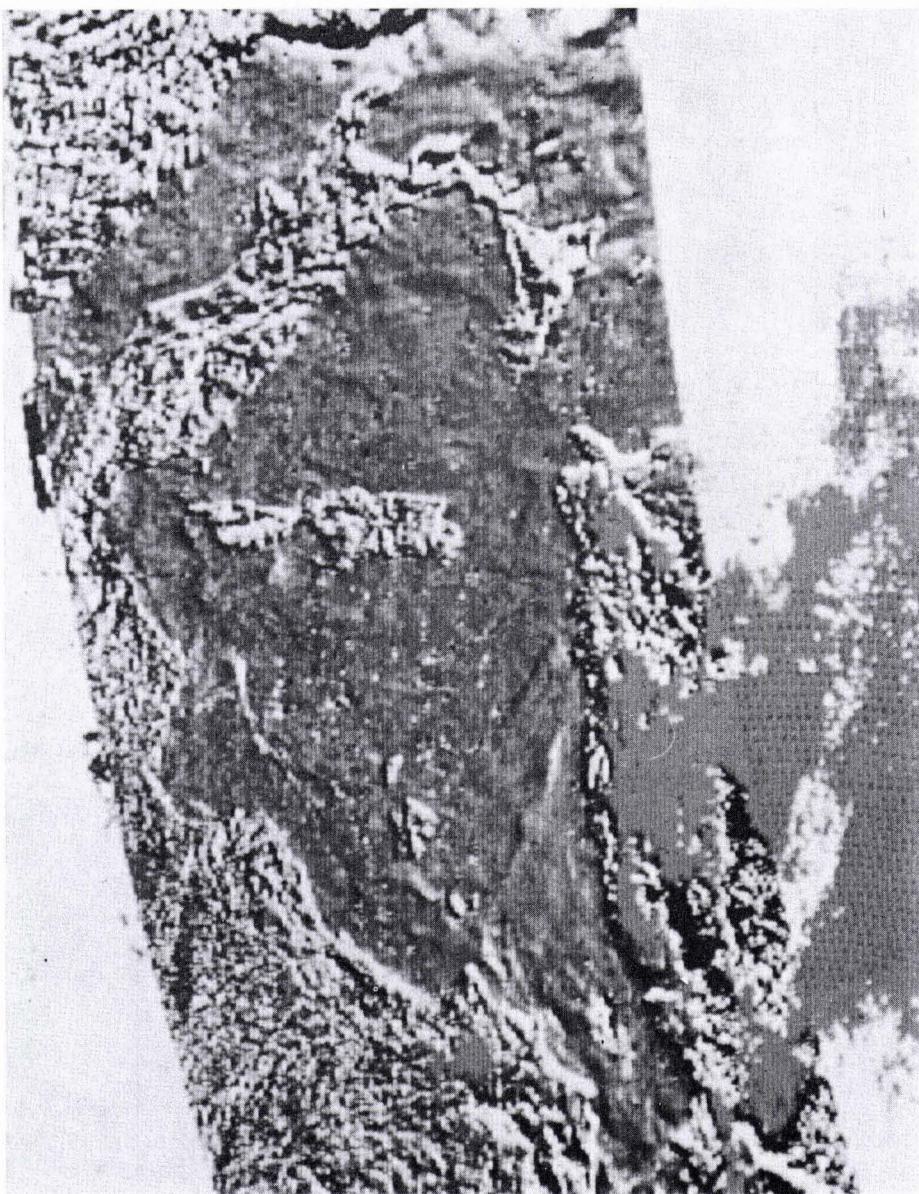


Figure 4. A difference image between mapped images based on the APT and HRPT data format. One pixel is equivalent to 4 km at 41° N (northern Sardinia).

white. The geographical goodness-of-fit is best seen along the coastline because of its high contrast in the original images.

A profile taken from each mapped image through the sunglint pattern is shown in figure 5. As a further direct comparison, the histograms of data within an irregularly shaped area east of Sardinia were plotted and first-order statistics calculated. Results were also calculated for the mapped APT images treated with a median filter having a 3×3 pixel window. The results are tabulated in table 2.

3. Discussion

The APT-formatted data are a subset of two of the five channels supplied by HRPT data. Thus they cannot supply the same amount of information. The advantages of using them lie in the relatively low cost and in the small size of the receiving equipment. This is of limited importance to research, however, unless the data can be accurately quantified. The two channels of data chosen for APT formatting have been until now the near-infrared (0.73 to 1.10 microns) and one thermal infrared (10.3 to 11.3 microns). The calibration of the visible and near-infrared channel sensors are assumed to remain constant at values supplied by NASA. Only the calibration of the thermal channels is discussed here.

The relationship between the radiance received by the sensor and the temperature of the emitting body is a function of the emissivity, the Planck function, and the wavelength response of the sensor. There is a non-linear dependence of radiance on temperature in the Planck function. Therefore to determine temperature from a measured radiance, it is computationally more efficient to determine an equation for $T=f(R)$, where $f(R)$ is a function of radiance over a limited temperature range. Calculations in this paper were done with the equation

$$T(^{\circ}\text{C}) = 1.1036R - 0.002376R^2 - 67.42$$

for R , the measured radiance, in $\text{mW}/(\text{sr} \cdot \text{m}^2/\text{cm})$. This equation was determined by an orthonormal polynomial fit over the temperature range 0°C to 20°C . Extrapolating this to the warmer temperatures encountered in the summer in the Mediterranean led to errors (for example, 0.08°C at 23.4°C). This does not affect the comparison of data, but a better equation for summer conditions would have been

$$T(^{\circ}\text{C}) = 0.9956R - 0.001798R^2 - 62.43$$

This is correct within 0.02°C over the range 10°C to 30°C for the 10.3 micron channel of NOAA-7.

The results of injecting a hypothetical count value (T_R) shows very clearly that the sensor data can be calibrated correctly from APT data. The average difference in the estimated temperatures is 0.09°C ($\sigma=0.07^{\circ}\text{C}$). The values in the T_L column were calculated on the basis of modelling the conversion of APT counts to HRPT counts as a linear process. The values at the nine modulation levels were fitted to the hypothetical values by linear least-squares fitting. The calculated correlation coefficient r^2 was 1.000, indicating very high linearity. However, the calculated temperature values (T_L) were in error by an average of 0.5°C ($\sigma=0.14$). Considering the residuals from the least-squares line it was apparent that the errors were largest at high and low modulation levels, just where the space and backscan values lay. Substituting the space-count value estimated by the polynomial fit into the calibration calculation from the linear model reduced the error to 0.1°C . The non-linearity of the amplitude modulation must be taken into account to attain accurate results.

A possible weakness in the APT calibration is the manner in which the calibration step levels are determined. The data are transmitted in an analogue form and subject to corruption by natural and man-made noise. At the location of the receiving system used the latter is probably the most damaging. To minimize the effects of noise spikes and bursts, the calibration algorithm selects the least noisy estimate (smallest standard deviation) for each of the space data and the 16 grey scale wedges over the image. Each estimate of the level of a wedge value is the average of 384 pixels. This is done separately for each channel and the final level estimates may not be exactly the same for the two channels. To estimate the effect of this, the thermometer count estimates of the near-I.R. channels were used in combination with the space and backscan values of the corresponding thermal channels to calibrate the instrument. The difference on the resulting T_R was insignificant (0.03°C , $\sigma=0.07$).

Figure 4 indicates that the APT data were mapped to the Mercator Projection to within 1 pixel (4 km at 41°N) over most of the image. The position error increased quickly in the south-east, being 16 km in the Gulf of Taranto. The reason for this is not yet clear, although the mapped pixels were from the ends of the scan lines in the original image.

A good deal of texture was evident in the land areas. Over land there is greater spatial detail and density of features emitting at different temperatures and with different emissivity. Thus small relative mapping errors were emphasized. Some of the pixels in the HRPT data that were resampled to produce an output at this scale were not present in the APT data. Also, since the data are intended for oceanographic use, temperature data beyond the expected sea surface temperature range were highly compressed and no attempt was made to maintain the same compression curves in the two data sets beyond the sea surface temperature range. This, combined with the extrapolation of the radiance to temperature curve beyond

TEMPERATURE , ALBEDO PROFILES THROUGH A SUN GLINT PATTERN

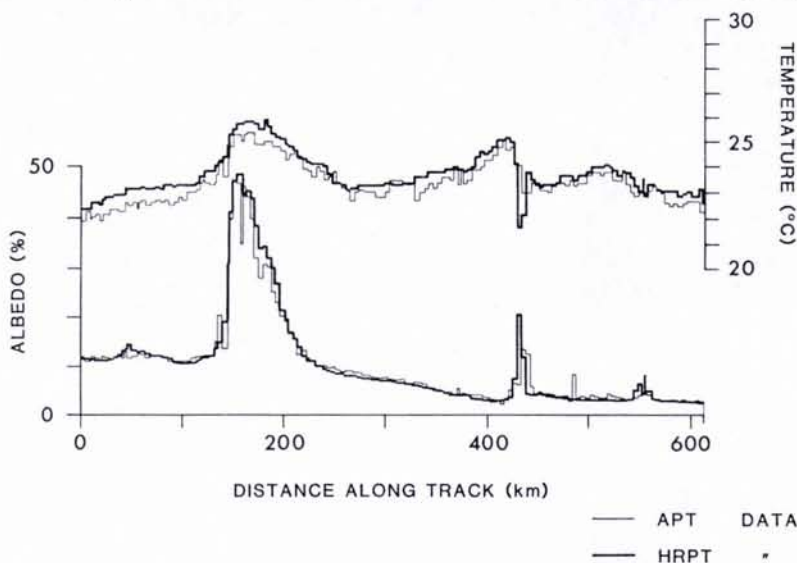


Figure 5 Profiles of equivalent black body temperature and percentage albedo along the same track in the four images mapped to the same scale.

its intended range, could result in temperature differences of a few degrees being calculated from similar count values. The more slowly varying structure in the sea surface values was due to the quantization of the APT data in the MIRP, and positional error.

An estimate of the error can be gained from the comparison profiles of figure 5. On average the thermal APT data were 0.31°C low along the length and the near-infrared albedo data were 0.1 per cent low. The forms of the profiles are consistent. The spike-like feature at about 430 km along the path is a narrow cloud streak that was partially smoothed by the lower resolution of the APT data.

A quantitative evaluation of the levels is shown in table 2, which presents the calculated statistics of the pixels in an area of 1147 pixels. The area was large enough to enclose surface temperature and albedo gradients and the data were thus not expected to exhibit gaussian distributions. For this reason also, the standard deviations of the data values may be larger than the noise levels of the sensors. The average near-infrared value is 0.2 per cent high and the standard deviation significantly higher (0.43 per cent as against 0.08 per cent) for the HRPT data. This is largely due to the noise spikes visible in the original image. Data reception at other geographical locations indicate that these spikes were predominantly due to nearby sources but this has yet to be investigated with simultaneous data reception. Such transients are however easily and quickly removed by median filtering (Huang *et al.* 1979) while leaving the positions and strengths of gradients unaltered. Filtering by replacing each pixel with the median of the nine surrounding pixels reduced the standard deviation to 0.18. The spike removal caused the histogram to become much less spread out along the albedo axis, the kurtosis was reduced from 155 to 4.

The average value of the APT infrared data was 0.27°C low. The higher order statistics of the median filtered image closely approached those of the HRPT image (standard deviation of 0.29° compared with 0.26°C). There were too few spikes to affect the average value. Over small areas the median value should be a better estimate of the true average than the calculated average in the presence of spikes, although the resolution of the estimate is limited to 0.1°C, which is the width of a histogram cell.

Table 2. A comparison of the statistical parameters calculated from an area of 1142 pixels in the images of NOAA-7 orbit 5379 mapped from APT and HRPT formatted data and from the APT image median filtered.

	Near I.R.		Thermal I.R.	
	Unfiltered	Filtered	Unfiltered	Filtered
Median (APT)	2.2	2.2	21.6	21.6
(HRPT)	2.1		21.8	
Average	2.27	2.28	21.57	21.57
	2.08		21.84	
Standard deviation	0.43	0.18	0.88	0.29
	0.08		0.26	
Skewness	4.41	2.00	2.85	1.23
	7.20		1.66	
Kurtosis	154.58	4.27	195.47	3.36
	27.16		4.15	

Starting with the NOAA-8 satellite the APT data transmission will consist of the near-I.R. and thermal I.R. channels during the day and two thermal I.R. channels at night. This will allow atmospheric correction algorithms to be used to derive estimates of the absolute sea surface temperature.

4. Conclusions

The results of an evaluation of the quality of meteorological satellite analogue APT transmissions have been discussed. The digitally transmitted data were taken as the standard of comparison; the analogue data were digitized immediately upon reception and analysed digitally. From the APT data the infrared sensor of the spacecraft could be calibrated within 0.1°C . The non-linearity of the transmission and data handling path had to be considered. Comparing the data from one satellite pass, the thermal data for sea surface temperature was about 0.3°C low. The albedo data agreed to within 0.2 per cent. The correction of panoramic distortion on board the spacecraft is a hindrance to mapping the APT data. The data were however mapped to an overall accuracy of one resolution cell (4 km). Mapping data from the ends of the sensor scan lines was less precise. The digital analysis of the APT data offers good-quality quantitative measurements for mesoscale oceanographic and meteorological research. Its advantages over the higher quality HRPT data are its lower cost and faster access time. It can be available on board ships and aircraft and in remote locations to steer experimental programmes in real time.

Acknowledgments

Essential to the retrieval of quantitative information from the high quality data supplied by NOAA in the APT format has been the hardware support by O. Chiappini, P. Guerrini and P. Lorenzelli and software support by P. Boni, A. Forber and P. Kitchen. The assistance of R. Seynaeve, E. Nacini and R. Giglione is also acknowledged.

References

- CARON, R. H., and SIMON, K. W., 1975, Attitude time-series estimates for rectification of spaceborne imagery. *J. Spacecraft Rockets*, **12**, 27–32.
- HUANG, T. S., YANG, G. J., and TANG, G. Y., 1979, A fast two-dimensional median filtering algorithm. *I.E.E.E. Trans. Acoust. Speech Signal Process.*, **27**, 13–18.
- LAURISTON, L., NELSON, G., and PORTO, F., 1979, Data extraction and calibration of TIROS-N/NOAA radiometers. NOAA TM NESS, TM 107, National Oceanic and Atmospheric Administration, Washington, D.C.
- LA VIOLETTE, P. E., STUART, L. JR., and VERMILLION, C., 1975, Use of APT satellite infrared data in oceanographic survey operations. *EOS, Trans. Am. geophys. Un.*, **56**, 276–282.
- ORTH, R., WONG, F., and MACDONALD J. S., 1978, The production of 1:250 000 maps of precision rectified and registered Landsat imagery using the MDA Image Analysis System: Initial results. In *Proceedings 12th Symposium Remote Sensing of Environment* (Ann Arbor, Michigan: Environmental Institute of Michigan), pp. 2163–2176.
- SCHWALB, A., 1978, The TIROS-N/NOAA A–G satellite series. NOAA TM NESS 95, National Oceanic and Atmospheric Administration, Washington, D.C.
- SCHWALB, A., 1982, Modified-version of the TIROS-N/NOAA-A, G satellite series: NOAA-E, -J Advanced TIROS-N (ATN). NOAA TM NESS 116, National Oceanic and Atmospheric Administration, Washington, D.C.
- Zwatz-Meiss, V., 1981, Use of satellite images and derived parameters for weather analysis and forecast. In *Remote Sensing in Meteorology, Oceanography and Hydrology* (edited by A. P. Cracknell (Chichester: Ellis Horwood), pp. 412–451.

INITIAL DISTRIBUTION

	Copies		Copies
<u>MINISTRIES OF DEFENCE</u>		<u>SCNR FOR SACLANTCEN</u>	
JSPHQ Belgium	2	SCNR Belgium	1
DND Canada	10	SCNR Canada	1
CHOD Denmark	8	SCNR Denmark	1
MOD France	8	SCNR Germany	1
MOD Germany	15	SCNR Greece	1
MOD Greece	11	SCNR Italy	1
MOD Italy	10	SCNR Netherlands	1
MOD Netherlands	12	SCNR Norway	1
CHOD Norway	10	SCNR Portugal	1
MOD Portugal	2	SCNR Turkey	1
MOD Spain	2	SCNR U.K.	1
MOD Turkey	5	SCNR U.S.	2
MOD U.K.	20	SECGEN Rep. SCNR	1
SECDEF U.S.	68	NAMILCOM Rep. SCNR	1
<u>NATO AUTHORITIES</u>		<u>NATIONAL LIAISON OFFICERS</u>	
Defence Planning Committee	3	NLO Canada	1
NAMILCOM	2	NLO Denmark	1
SACLANT	10	NLO Germany	1
SACLANTREPEUR	1	NLO Italy	1
CINWESTLANT/COMOCEANLANT	1	NLO U.K.	1
COMSTRIKFLTANT	1	NLO U.S.	1
COMIBERLANT	1		
CINCEASTLANT	1	<u>NLR TO SACLANT</u>	
COMSUBACLANT	1	NLR Belgium	1
COMMAIREASTLANT	1	NLR Canada	1
SACEUR	2	NLR Denmark	1
CINCNORTH	1	NLR Germany	1
CINCSOUTH	1	NLR Greece	1
COMNAVSOUTH	1	NLR Italy	1
COMSTRIKFORSOUTH	1	NLR Netherlands	1
COMEDCENT	1	NLR Norway	1
COMMARAIRED	1	NLR Portugal	1
CINCHAN	3	NLR Turkey	1
		NLR UK	1
		NLR US	1
		Total initial distribution	249
		SACLANTCEN Library	10
		Stock	21
		Total number of copies	280